Available online at www.sciencedirect.com
ScienceDirect
Journal of the European Ceramic Society 29 (2009) 125–130
www.elsevier.com/locate/jeurceramsoc

Effect of pH on the production of dispersed $Bi_4Ge_3O_{12}$ nanoparticles by combustion synthesis

Fabiane Alexsandra Andrade de Jesus [a], Ronaldo Santos Silva [a], Antonio Carlos Hernandes [b], Zélia Soares Macedo [a,*]

[a] *Grupo de Materiais Cerâmicos Avançados, Departamento de Física, Universidade Federal de Sergipe, Campus Universitário, 49.100-100 São Cristóvão, SE, Brazil*

[b] *Grupo Crescimento de Cristais e Materiais Cerâmicos, Instituto de Física de São Carlos, Universidade de São Paulo, CP 369, 13560-970 São Carlos, SP, Brazil*

Received 30 January 2008; received in revised form 26 May 2008; accepted 30 May 2008
Available online 23 July 2008

Abstract

This paper reports the production of bismuth germanate ceramic scintillator ($Bi_4Ge_3O_{12}$) by combustion synthesis (SHS) method, focusing on the influence of the synthesis parameters on the crystalline phases and agglomeration of the nanoparticles. The synthesis and sintering conditions were investigated through thermal analysis, X-ray diffraction as function of temperature, dilatometry and scanning electron microscopy. Well-dispersed $Bi_4Ge_3O_{12}$ powder was accomplished by the combustion of the initial solution at pH 9, followed by low temperature calcination and milling. Sintered ceramics presented relative density of 98% and single crystalline $Bi_4Ge_3O_{12}$ phase. The luminescent properties of the ceramics were investigated by photo- and radio-luminescence measurements and reproduced the typical $Bi_4Ge_3O_{12}$ single-crystal spectra when excited with UV, β and X-rays. The sintered ceramics presented light output of 4.4×10^3 photons/MeV.

Keywords: Combustion processing; Grain size; Luminescence; $Bi_4Ge_3O_{12}$; Scintillator applications

1. Introduction

Bismuth germanate ($Bi_4Ge_3O_{12}$—BGO) is a scintillator material used as single crystal in medical detectors and high energy physics. $Bi_4Ge_3O_{12}$ presents several advantages such as high density, good stability, low afterglow, high light output (9×10^3 photons/MeV for single crystal) and good sensibility to a great variety of energies (UV, α, β and γ radiation).[1–4] The use of $Bi_4Ge_3O_{12}$ ceramics in detector devices would bring additional advantages in cost production, versatility of shapes and sizes and homogeneous distribution of the dopands.[5,6] However, ceramics normally scatter light, which reduces the efficiency of the scintillator. Since porosity is the main factor producing light scattering, high densification and pore elimination are important advances for the potential use of BGO ceramics as radiation detectors. Dense ceramics can be reached from compacts of nanoparticles that present high effective area and high surface energies. Consequently, the grain boundary mobility and the sinterability increase for nanostructured ceramics, when compared to compacts of micrometric particles.

Self-propagating high-temperature synthesis (SHS—combustion synthesis) involves high temperatures induced by a self-sustained exothermic reaction of a fuel mixed to the reactants. It has been investigated for many compounds and became a powerful technology to produce inorganic materials.[7–9] Typically, SHS route produces nano-sized particles, but it also results in a high degree of agglomeration of these particles. Agglomeration can reduce the final density of the sintered ceramic, since intra- and inter-agglomerate sintering does not occur simultaneously. On the other hand, there are reports on the influence of the pH on the agglomeration degree and morphology of the particles produced by wet chemistry[10,11] and also by SHS route.[12,13] All these reports point out pH control as an efficient method to change the agglomeration degree and, in some cases, also the particle size and morphology.

In this work we have studied by the first time the production of nanostructured $Bi_4Ge_3O_{12}$ powders via SHS. This compound is traditionally produced through solid state route,[5,6,14–16] which is

* Corresponding author.
E-mail address: zmacedo@fisica.ufs.br (Z.S. Macedo).

0955-2219/$ – see front matter © 2008 Published by Elsevier Ltd.
doi:10.1016/j.jeurceramsoc.2008.05.048

time-expensive and presents micrometric particles with a small amount of spurious phase $Bi_{12}GeO_{20}$. We also report here the influence of pH on the crystalline phases and agglomeration of the nanoparticles produced by SHS, and show that the good dispersion of the particles lead to sintered ceramic bodies with higher density.

2. Experimental

SHS route consists in heating a mixture of metal salts, oxides and/or carbonates and a suitable organic fuel, until it ignites and a self-sustaining and rather fast combustion reaction takes off. For the combustion synthesis of bismuth germanate, the cationic precursors used were GeO_2 (Alfa Aesar, 5N) and $Bi(NO_3)_3{\cdot}5H_2O$ (Alfa Aesar, 98%), using CON_2H_4 (urea) (VETEC, P.A.) as fuel. The following equation describes the chemical reaction involved in the synthesis[9]:

$$4Bi(NO_3)_3{\cdot}5H_2O + 3GeO_2 + 10CON_2H_4 \rightarrow Bi_4Ge_3O_{12} + 10CO_2 + 32N_2 + 25H_2O \quad (1)$$

The stoichiometric composition of the redox mixture for combustion synthesis was calculated based on the total oxidizing and reducing valences of the oxidizer and the fuel. The precursors were mixed with a small quantity of distilled water in an alumina crucible and stirred in order to obtain a homogeneous paste. This paste presented initially pH 1 due to the acidity of $Bi(NO_3)_3{\cdot}5H_2O$ solution in water. To adjust pH, ammonium hydroxide (NH_4OH; QUIMEX, P.A.) was used instead of water. The pH values studied were 1 (without NH_4OH), 5, 7, 9 and 11. The synthesis was carried out by heating this mixture on an electric plate at 500 °C. At this temperature, the exothermic decomposition of the fuel took place, leading to an enhancement of the temperature and the reaction between the precursors.

After the combustion reaction, two distinct procedures were adopted: (i) the reacted powders were pressed and sintered; (ii) the reacted powders were calcined at 600 °C/24 h, ball-milled for 24 h, pressed and sintered. The ball-milling was made in plastic recipients containing the powders, zirconia balls and isopropyl alcohol, in the volumetric proportion of 10:60:30, respectively. In both procedures the samples were conformed by uniaxial pressing and sintered at 840 °C/3 h, with a heating rate of 10 °C/min and a cooling rate of 2 °C/min. The relative density of the sintered ceramics was determined by the fluid displacement (Archimedes) method using distilled water.

Thermal analysis of the powders employed a simultaneous TG/DTA (STA 409 Netzsch) system and the measurements were made from room temperature up to 1100 °C with heating rate of 10 °C/min under synthetic air flow. Dilatometric measurements (dilatometer Netzsch—402 PC) were performed in a temperature range from 25 °C to 950 °C, with a heating rate of 10 °C/min in synthetic air flow.

The crystalline phases of the powder and sintered ceramics were inspected by X-ray diffraction (XRD; Rigaku RINT 2000/PC) technique, in continuous scanning mode using Cu Kα radiation, in the 2θ range between 10° and 80°. XRD measurements as a function of the temperature employed a HTK 1200 furnace (Anton Paar) coupled to the diffractometer. The experimental XRD patterns were compared to the data from JCPDS (Joint Committee on Powder Diffraction Standards, Swarthmore, USA).

The particle size of the reacted powders was determined by a Zetasizer Malvern Nano Series, at room temperature, after dispersion of the powders for 1 h in an ultrasonic bath. The agglomeration of these powders and also the microstructure of the sintered ceramics were analyzed by scanning electron microscopy (SEM; Zeiss DSM960).

The luminescence properties of the samples were inspected via photo- and radioluminescence techniques at room temperature. The photoluminescence (PL) spectra of the scintillators were measured by a Ocean Optics HR 2000 spectrometer (resolution of 0.5 nm) under excitation of a 300-W Xenon lamp.

Radioluminescence (RL) was measured under excitation of both X-rays and β particles. Under irradiation with X-rays (∼9 keV), RL was registered using the same spectrometer used in the PL tests. For RL measurements under β radiation, $Bi_4Ge_3O_{12}$ ceramics were exposed to a $^{90}Sr/^{90}Y$ source, with dose rate of 0.2 Gy/min at the sample position. In this case, the light emitted during the irradiation was detected by a Hamamatsu R928 photomultiplier tube attached to a monochomator (FUNBEC, Unicrom 100), with 5 nm resolution. The electric current of the photomultiplier was registered using a Keithley 6517 electrometer.

3. Results and discussion

The samples produced with pH 1, 5, 7, 9 and 11 will be called, respectively, BGO1, BGO5, BGO7, BGO9 and BGO11 hereafter. Fig. 1 presents the XRD patterns of the as-prepared powders. For BGO1, the major phases detected in the reacted powder were GeO, GeO_2 and Bi_2O_3. These same phases were also observed in both BGO5 and BGO7 samples, with slight

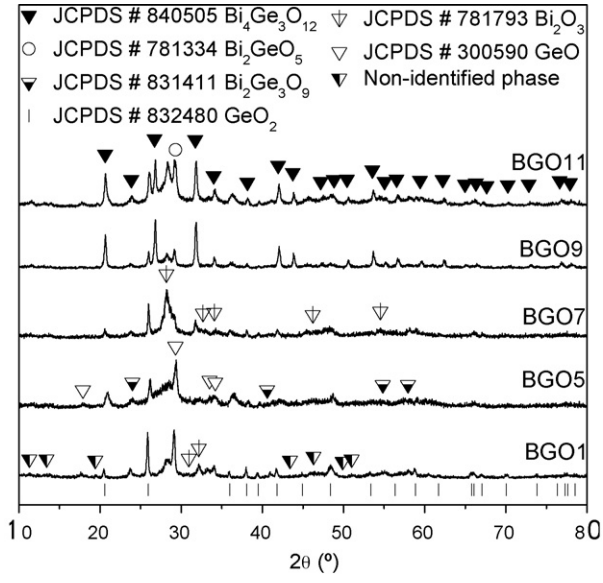

Fig. 1. XRD patterns of the as-prepared powders with different pH values: BGO1, pH 1; BGO5, pH 5; BGO7, pH 7; BGO9, pH 9; BGO11, pH 11.

variations in the relative amounts. On the other hand, $Bi_4Ge_3O_{12}$ was the major phase in BGO9. For this sample, small amounts of the phases GeO_2, Bi_2GeO_5 and a non-identified phase have also been observed. For BGO11, the peaks corresponding to the phases GeO_2 and Bi_2GeO_5 increased relatively to the peaks of the $Bi_4Ge_3O_{12}$ phase. The absence of bismuth germanate in BGO1, BGO5 and BGO7 indicates a dependency of the urea decomposition on the bulk pH. Since NH_4OH, used to adjust pH, also undergoes exothermic decomposition when heated, it could be supposed that the phase formation is due to higher densities of energy delivered to the mixture with higher pH. To test this hypothesis, further SHS reactions employing excess of urea and without pH adjustments were performed. The results from these tests were the same of that presented in Fig. 1 for BGO1, so it could be concluded that the pH of the initial mixture plays a determinant role on the formation of crystalline phases, regardless the excess of fuel used for the reaction. Since SHS is a redox reaction, it is possible that higher concentrations of $(OH)^-$ groups in the mixture result in an enhancement on the rate of decomposition of urea. The energy liberated in a shorter time interval would provide higher temperatures for the reaction.

Considering that the powder produced at any pH could possibly reach single phase under additional calcinations, as reported by several authors,[9,17] and also that the simultaneous calcination and sintering would prevent grain growth and in some cases would result in high density,[18] all the produced powders were tested in a simultaneous calcination and sintering stage at 840 °C for 3 h. As expected, all the sintered ceramics presented $Bi_4Ge_3O_{12}$ as single or major phase (illustrated in Fig. 2 for BGO9 sample) with very small amounts of $Bi_{12}GeO_{20}$ which sometimes stayed below the accuracy of XRD measurements. Nevertheless, the samples without the initial phase $Bi_4Ge_3O_{12}$ presented poor density, as explained below.

DTA curve, presented in Fig. 2b, confirms the structure of the produced material. The endothermic peaks at 880 °C and 1050 °C correspond, respectively, to the euthetic point, in which the liquid phase coexists with the crystalline phases $Bi_4Ge_3O_{12}$ and $Bi_{12}GeO_{20}$, and to the melting point of $Bi_4Ge_3O_{12}$.[19]

Fig. 3 presents the particle size distribution of the reacted powders, obtained via Zetasizer measurements. The mean size determined in this graph was 100 ± 30 nm. No significant pH influence on the particle size was observed in these measurements. On the other hand, the samples presented remarkable differences concerning to the agglomeration degree, as can be verified in Fig. 4. The combustion reaction without pH adjustment produced a strongly agglomerated material (see Fig. 4a), whereas the powder produced at alkaline environment was well dispersed, as shown in Fig. 4b.

The good dispersion of the powders is determinant of ceramic sinterability, as can be verified by the comparison of the relative densities of the sintered ceramics, presented in Table 1. The powders produced at acid conditions (strongly agglomerated) yielded ceramic bodies with relative densities between 68% and 73%. For the less agglomerated samples BGO9 and BGO11, produced at alkaline pH values, the final density of the sintered ceramics was 84–87%.

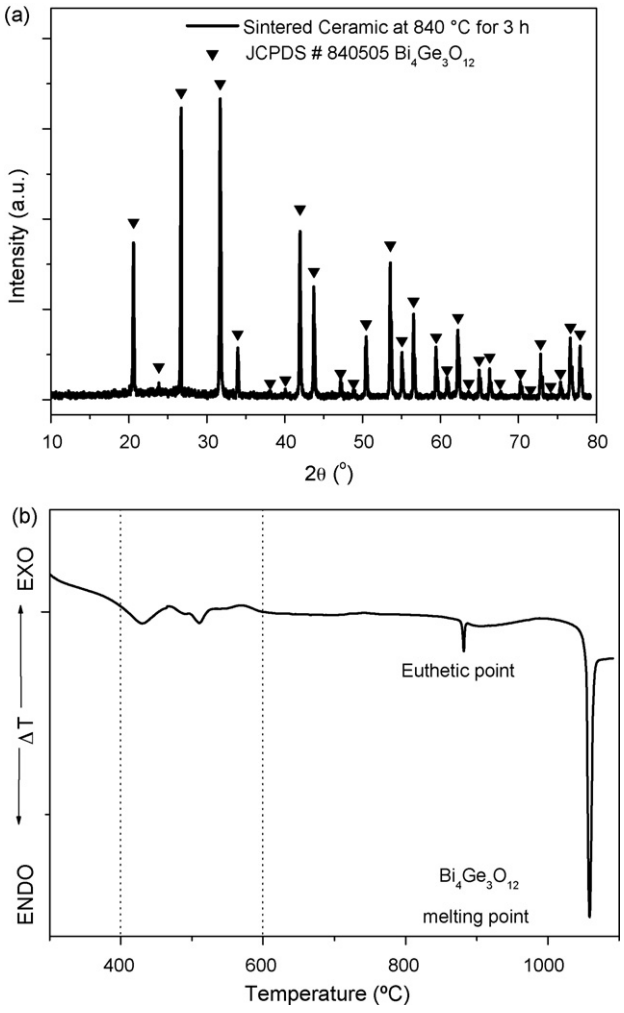

Fig. 2. Structural and thermal characterization of BGO9 sample: (a) XRD pattern of the ceramic sintered at 840 °C for 3 h without intermediate calcination; (b) DTA curve of the as-prepared BGO9.

Fig. 5a presents the linear shrinkage ($Y = \Delta L/L_0$) and the linear shrinkage rate (dY/dT) of the BGO1 sample as a function of the temperature. Clearly, this curve exhibits a non-conventional behavior for ceramic materials presenting two distinct shrink-

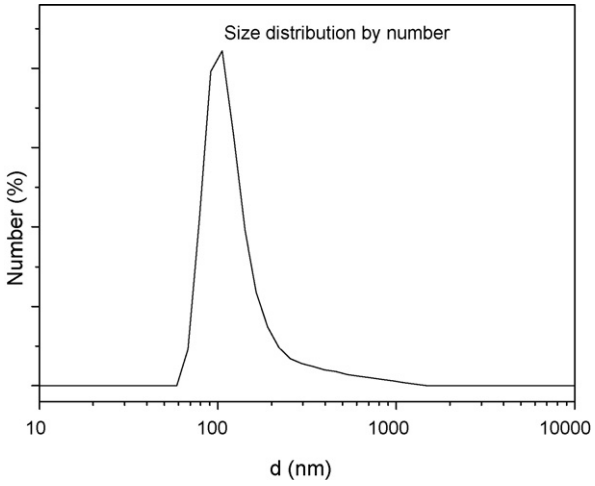

Fig. 3. The size distribution graph of BGO1.

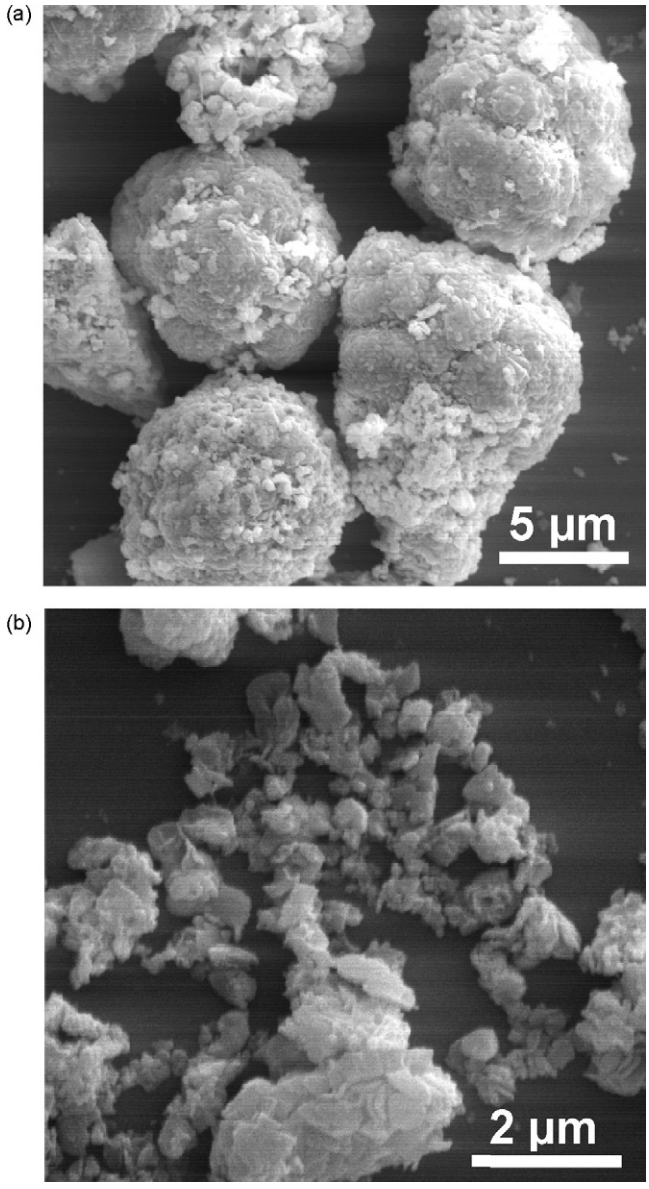

Fig. 4. SEM micrographs of the as-prepared powder: (a) BGO1; (b) BGO9.

age processes. In the first one, the shrinkage begins at 480 °C and presents a maximum rate at 525 °C. This event occurs due to the elimination of remaining sub-products, also registered in the DTA graph (see Fig. 2b), between 400 °C and 600 °C. The second process begins at 780 °C and presents two inflection points at 847 °C and 896 °C which are related to intra- and inter-agglomerates sintering, respectively. The coalescence

Table 1
Relative density of the BGO ceramics sintered at 840 °C/3 h

Sample	Relative density (%)
BGO1	68 ± 1
BGO5	61.3 ± 0.3
BGO7	73.0 ± 0.5
BGO9	87.0 ± 0.5
BGO11	84.0 ± 0.3

The theoretical density of BGO is $\rho_0 = 7.13\ g/cm^3$.

of intra-agglomerate particles at temperatures lower than the inter-agglomerate sintering results in ceramic bodies with high porosity, as can be seen in the micrograph at Fig. 5b for ceramic bodies sintered at 840 °C for 3 h. Although the maximum shrinkage rate was observed at 896 °C, this temperature was not tested for sintering, since it is only 50 °C below the melting point of $Bi_4Ge_3O_{12}$.

From the results presented up to this point, we can conclude that pH 9 is the optimum value to obtain the best result on the $Bi_4Ge_3O_{12}$ production via combustion synthesis. However, the density of 87% (Table 1) reached by the ceramics submitted to simultaneous sintering and calcinations is yet quite low. In order to enhance the final density of the sintered ceramics, a new procedure, with separated stages of calcination and sintering, was tested. To determine the optimum temperature for calcinations, the crystalline phase evolution was monitored by XRD measurements performed at different temperatures during the heating of the sample. Fig. 6 presents these results and it can be

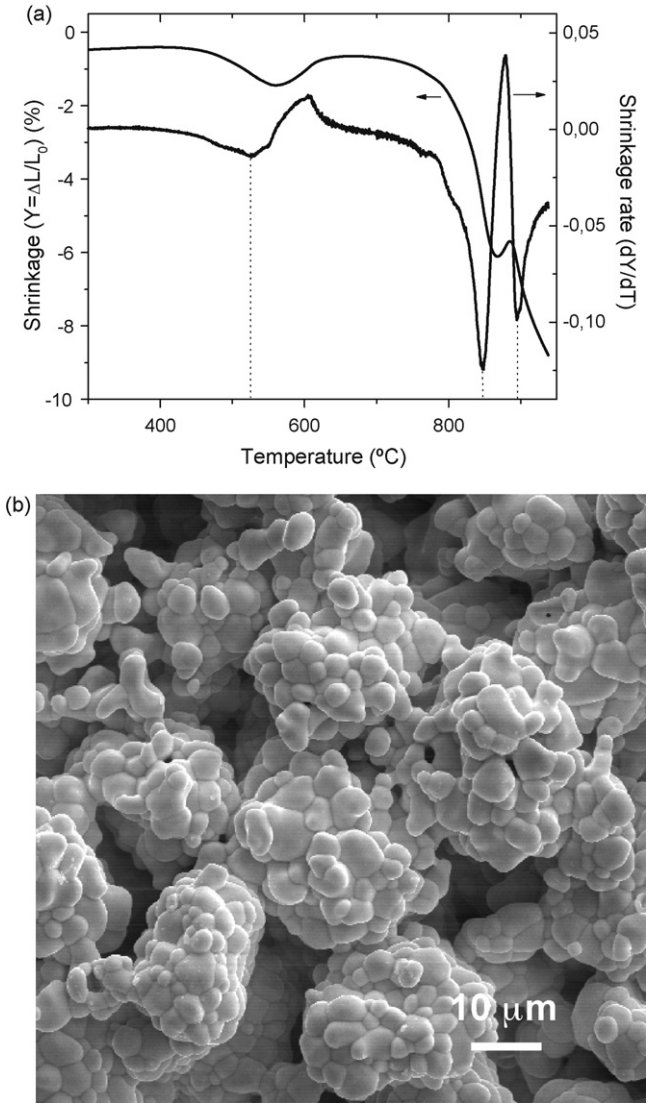

Fig. 5. BGO1 sample: (a) linear shrinkage and shrinkage rate as a function of the temperature; (b) SEM micrograph of BGO1 sintered at 840 °C for 3 h.

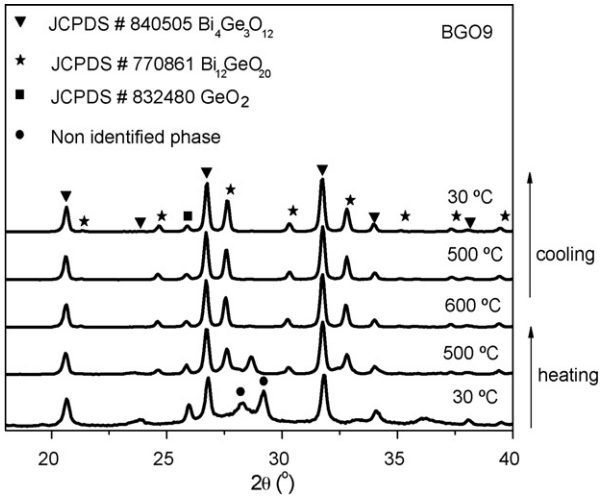

Fig. 6. XRD patterns of the BGO9 sample measured during the calcination process.

observed that $Bi_4Ge_3O_{12}$ peaks kept the same relative intensity during the heating, whereas the non-identified phase was eliminated by the calcination. At 600 °C, the non-identified phase was completely eliminated, but the formation of the $Bi_{12}GeO_{20}$ phase at 500 °C was also observed. The elimination of the non-identified phase and the formation of the $Bi_{12}GeO_{20}$ phase are related to the endothermic peaks between 400 °C and 600 °C registered in DTA curve of Fig. 2b. The $Bi_{12}GeO_{20}$ phase was already reported in the production of $Bi_4Ge_3O_{12}$ via solid-state synthesis[20] and it was also observed in small quantities in the sintered bodies in the present work.

Since the temperature necessary to reduce the quantity of $Bi_{12}GeO_{20}$ would be too close to the sintering temperatures, the calcination was performed at 600 °C, which is the lowest temperature necessary to eliminate the unknown phase and to reduce considerably the presence of GeO_2 (Fig. 6). The powders calcined at 600 °C/24 h presented the major phase $Bi_4Ge_3O_{12}$. In order to prevent the particle coalescence, an additional ball-milling process for 24 h after the calcination was adopted.

Fig. 7a presents the dilatometric analysis of the BGO9 sample calcined at 600 °C and ball-milled for 24 h. This curve does not present any shrinkage due to elimination of sub-products, intra-agglomerate sintering or any other process that would interfere with the quality of the final density. A single shrinkage process was observed, with onset at 700 °C and maximum shrinkage rate at around 840 °C. The relative density ρ/ρ_0, calculated from the shrinkage values $\Delta L/L_0$ by the expression $\rho/\rho_0 = (1 - \Delta L/L_0)^{-3}$, was 95% at 875 °C, as presented in Fig. 7a. According to these results, the optimum sintering temperature for BGO9 is 840 °C.

The samples sintered at 840 °C for 3 h reached a final density of 98%. Fig. 7b presents the SEM image of the sintered body, with low porosity, homogeneous microstructure with an average grain size of 5 μm. This sample was chosen for the luminescence study.

The luminescence curves of the ceramics under β, X-rays and ultraviolet (UV) excitation are presented in Fig. 8. In all the cases, it was observed a broad emission band with maxima positions at 510, 515 and 520 nm, for irradiation with β, X-rays and UV, respectively. These peak positions are the same, considering the experimental deviation, and corroborate the values found in the literature.[5] Luminescence emission in $Bi_4Ge_3O_{12}$ is associated to Bi^{3+} transitions from the excited level 6p6s ($^3P_{0,1,2}$, $^1P_1$) to the fundamental state $6s_2$ ($^1S_0$). From the curves of Fig. 8 it can be concluded that the same luminescence centers are activated by all the studied energies, and that no additional luminescence center was created due to the combustion synthesis route.

The relative light output of the scintillators can be obtained directly from the area under the RL curve. For comparison, the efficiency of BGO single crystal was measured under β and X-rays excitation. When compared to the BGO single crystal (9×10^3 photons/MeV at 300 K[1,20,21]), the sintered ceramics presented an energy efficiency of

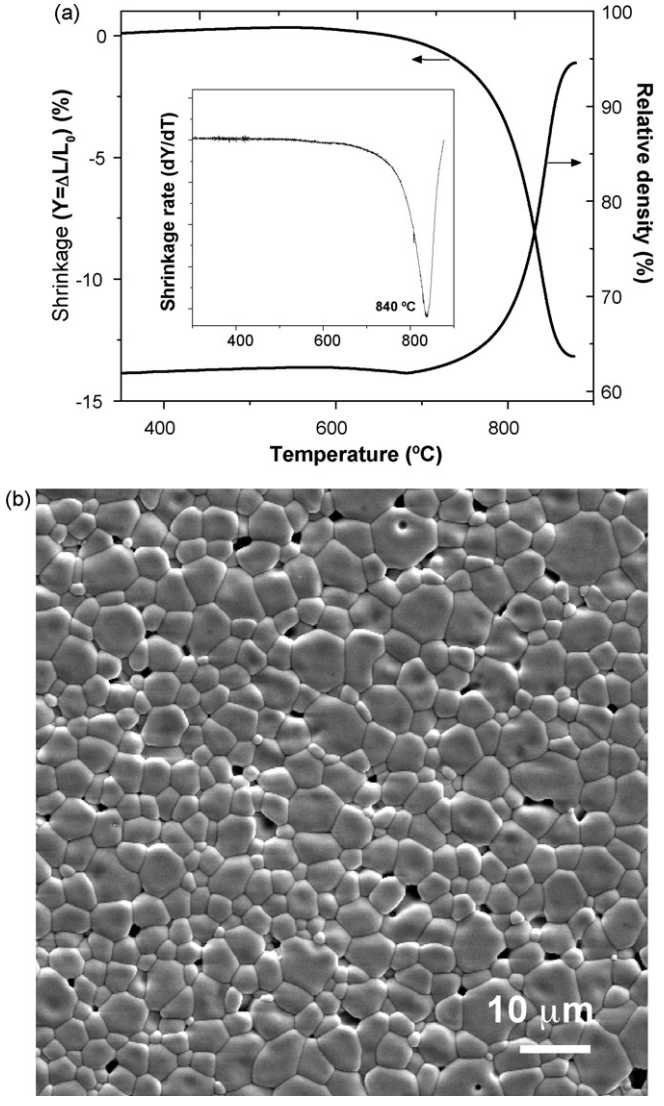

Fig. 7. Dilatometric analysis of BGO9 sample calcined at 600 °C and ball-milled for 24 h: (a) linear shrinkage (Y) and relative density (inset shows linear shrinkage rate); (b) SEM micrograph of BGO9, after calcinations (600 °C/24 h), ball-milling (24 h) and sintering (840 °C/3 h). The relative density is $\rho_{rel} = 98.1 \pm 0.5\%$.

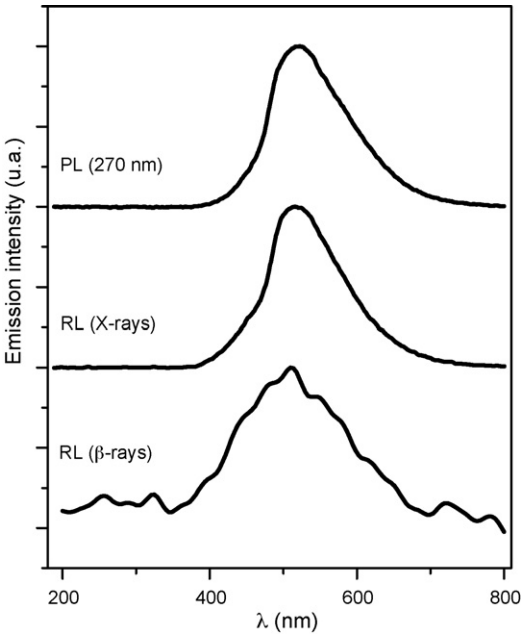

Fig. 8. Luminescence spectra of $Bi_4Ge_3O_{12}$ ceramics under β, X-rays and ultraviolet (UV) excitation.

4.4×10^3 photons/MeV. This value is comparable to the light output from CeF_3 single crystal (4×10^3 photons/MeV) and $BaHfO_3$:Ce ceramics (6×10^3 photons/MeV), and satisfies the requirement for application in electromagnetic calorimeters that is 200 photons/MeV.[1,20]

4. Conclusions

Bismuth germanate ceramic powders were successfully synthesized by the first time through SHS route. The pH control associated with calcination and milling stages were important factors to reduce the agglomeration degree in the synthesized powders and to enhance the final density of the sintered ceramics. The optimum synthesis conditions were determined as pH = 9 during the reaction, and calcination (600 °C/24 h) and ball-milling (24 h) procedures after the combustion. The powders resulting from this synthesis route presented $Bi_4Ge_3O_{12}$ as the major phase and weak agglomeration of the nanoparticles. Ceramics sintered at 840 °C/3 h reached a final relative density of 98% and homogeneous microstructure. The luminescence spectra of the ceramics excited with UV, β and X-rays reproduced the typical $Bi_4Ge_3O_{12}$ single crystal behavior with emission bands centered about 515 nm, indicating that this new route did not affect the luminescent centers of the material. The sintered ceramics presented light output of 4.4×10^3 photons/MeV, which is comparable to that presented by the BGO single crystal and satisfies the requirement for application in electromagnetic calorimeters.

Acknowledgements

The authors wish to acknowledge Eduardo Antonelli for the SEM micrographs and CAPES, CNPq, Ceramica Sergipe s/a, UFS and FINEP for the financial support.

References

1. Blasse, G., Scintillator materials. *Chem. Mater.*, 1994, **6**, 1465–1475.
2. van Eijk, C. W. E., Inorganic scintillators in medical imaging. *Phys. Med. Biol.*, 2002, **47**, R85–R106.
3. Grabmaier, B. C., Luminescent materials for medical application. *J. Lumin.*, 1994, **60 & 61**, 967–970.
4. Longo, E., 25 years of scintillating crystal in high-energy physics. *Nucl. Instrum. Methods*, 2002, **486**, 7–12.
5. Macedo, Z. S., Silva, R. S., Valerio, M. E. G. and Hernandes, A. C., Radiation detectors based on laser sintered $Bi_4Ge_3O_{12}$ ceramics. *Nucl. Instrum. Methods B*, 2004, **218**, 153–157.
6. Santana, G. C., Mello, A. C. S., de Silva, R. S., Hernandes, A. C., Valerio, M. E. G. and Macedo, Z. S., Scintillating properties of pure and doped BGO ceramics. *J. Mater. Sci.*, 2007, **42**, 2231–2235.
7. Makino, A. and Law, C. K., SHS combustion characteristics of several ceramics and intermetallic compounds. *J. Am. Ceram. Soc.*, 1994, **77**, 778–786.
8. Moore, J. J. and Feng, H. J., Combustion synthesis of advanced materials. Part I. Reaction parameters. *Prog. Mater. Sci.*, 1995, **39**, 243–273.
9. Macedo, Z. S., Ferrari, C. R. and Hernandes, A. C., Self-propagation high-temperature synthesis of bismuth titanate. *Powder Technol.*, 2004, **139**, 175–179.
10. Silva, R. S., Bernardi, M. I. B. and Hernandes, A. C., Synthesis of non-agglomerated $Ba_{0.77}Ca_{0.23}TiO_3$ nanopowders by a modified polymeric precursor method. *J. Sol–Gel Sci. Technol.*, 2007, **42**, 173–179.
11. Luan, W. and Gao, L., Influence of pH value on properties of nanocrystalline $BaTiO_3$ powder. *Ceram. Int.*, 2001, **27**, 645–648.
12. Pathak, L. C., Singh, T. B., Das, S., Verma, A. K. and Ramachandrarao, P., Effect of pH on the combustion synthesis of nano-crystalline alumina powder. *Mater. Lett.*, 2002, **57**, 380–385.
13. Peng, T., Liu, X., Dai, K., Xiao, J. and Song, H., Effect of acidity on the glycine–nitrate combustion synthesis of nanocrystalline alumina powder. *MRS Bull.*, 2006, **41**, 1638–1645.
14. Macedo, Z. S. and Hernandes, A. C., Laser sintering of bismuth germanate ($Bi_4Ge_3O_{12}$) ceramics. *J. Am. Ceram. Soc.*, 2002, **85**(7), 1870–1872.
15. de Mello, A. C. S., Santana, G. C., Jackson, R. A., Macedo, Z. S., Moreira, S. G. C. and Valerio, M. E. G., Optical properties of pure and Cr^{3+} doped BGO ceramic scintillators. *Phys. Stat. Sol. (c)*, 2007, **4**(3), 980–983.
16. Macedo, Z. S., Silva, R. S., Valerio, M. E. G., Martinez, A. L. and Hernandes, A. C., Laser-sintered bismuth germanate ceramics as scintillator devices. *J. Am. Ceram.*, 2004, **87**(6), 1076–1081.
17. Sych, A. M., Nedilĭko, L. F. and kuzĭmin, R. N., Combustion synthesis of bismuth titanates and niobates. *Inorg. Mater.*, 1999, **35**(3), 290–294.
18. Macedo, Z. S., Ferrari, C. R. and Hernandes, A. C., Impedance spectroscopy of $Bi_4Ti_3O_{12}$ ceramic produced by self-propagating high-temperature synthesis technique. *J. Eur. Ceram. Soc.*, 2004, **24**, 2567–2574.
19. Smet, F. and Enckevort, W. J. P. V., In situ microscopic investigations of crystal growth processes in the system Bi_2O_3–GeO_2. *J. Cryst. Growth*, 1990, **100**(3), 417–432.
20. Greskovich, C. and Duclos, S., Ceramics scintillators. *Annu. Rev. Mater. Sci.*, 1997, **27**, 69–88.
21. Knoll, G. F., *Radiation Detection and Measurement*. John Wiley & Sons, New York, 1989, pp. 215–250.